Three-photon absorption in anthracene-porphyrin-anthracene triads: A quantum-chemical study

Lingyun Zhu, Xia Yang, Yuanping Yi, Pengfei Xuan, Zhigang Shuai, Dezhan Chen, Egbert Zojer, Jean-Luc Brédas, and David Beljonne

Citation: The Journal of Chemical Physics **121**, 11060 (2004); doi: 10.1063/1.1813437
View online: https://doi.org/10.1063/1.1813437
View Table of Contents: http://aip.scitation.org/toc/jcp/121/22
Published by the American Institute of Physics

Three-photon absorption in anthracene-porphyrin-anthracene triads: A quantum-chemical study

Lingyun Zhu
Laboratory of Organic Solids, Center for Molecular Sciences, Institute of Chemistry, The Chinese Academy of Sciences, 100080 Beijing, People's Republic of China and Department of Chemistry, Shandong Normal University, Jinan 250014, People's Republic of China

Xia Yang, Yuanping Yi, Pengfei Xuan, and Zhigang Shuai[a)]
Laboratory of Organic Solids, Center for Molecular Sciences, Institute of Chemistry, The Chinese Academy of Sciences, 100080 Beijing, People's Republic of China

Dezhan Chen
Department of Chemistry, Shandong Normal University, Jinan 250014, People's Republic of China

Egbert Zojer
School of Chemistry and Biochemistry, Georgia Institute of Technology, Atlanta, Georgia 30332-0400

Jean-Luc Brédas
School of Chemistry and Biochemistry, Georgia Institute of Technology, Atlanta, Georgia 30332-0400 and Service de Chimie des Matériaux Nouveaux, Université de Mons-Hainaut, B-7000 Mons, Belgium

David Beljonne
Service de Chimie des Matériaux Nouveaux, Université de Mons-Hainaut, B-7000 Mons, Belgium and School of Chemistry and Biochemistry, Georgia Institute of Technology, Atlanta, Georgia 30332-0400

(Received 16 February 2004; accepted 15 September 2004)

We have applied correlated quantum-chemical methods to investigate the three-photon absorption (3PA) response of a porphyrin triad derivative, where the central macrocycle is linked in mesopositions to two anthracene units via acetylenic bridges. The 3PA frequency-dependent spectrum of this derivative is dominated by a single resonance feature in the transparent region, associated with charge-transfer states between porphyrin and anthracene. The calculations indicate a two order of magnitude enhancement in the 3PA cross section in the triad molecule with respect to the individual entities, which is attributed to close one-, two-, and three-photon resonances together with strong electronic couplings among the units. © *2004 American Institute of Physics*. [DOI: 10.1063/1.1813437]

I. INTRODUCTION

Novel molecular and/or polymeric organic architectures with efficient multiphoton absorption (MPA) properties are desirable because of emerging applications notably in the fields of optical power limiting, frequency-upconverted fluorescence microscopy, photorefractivity, three-dimensional optical data storage, or two-photon photodynamic therapy.[1–7] Three-photon absorption (3PA) is a process in which an atom or a molecule simultaneously absorbs three photons, which, if possessing the same frequency, yield an excited state lying at three times the photon energy above the ground state. Compared to two-photon absorption (2PA), longer excitation wavelengths can be used in 3PA-based applications providing deeper penetration depths in scattering or absorbing media; in addition, the cubic dependence of the three-photon process on the input light intensity leads to a stronger spatial confinement, so that a higher imaging contrast can in principle be obtained. In spite of such intrinsic advantages, three-photon absorption has so far obtained limited attention, mostly as a result of the very low cross sections associated with such a fifth-order nonlinear optical process. Recently, experimental observations of 3PA effects have been reported in organic conjugated molecules.[2,8–11] However, there have been only few attempts to model the microscopic mechanisms for such processes[12–15] or to propose guidelines for the design of molecular architectures with enhanced 3PA cross sections.

It is well recognized that the origin for the large optical nonlinearities in conjugated organic systems arises from the presence of a highly delocalized π-electron cloud. This leads to low excitation energies and large dipole matrix elements, translating altogether into high nonlinear electrical polarizabilities, as readily seen from perturbation theory and a sum-over-states (SOS) picture.[16] Porphyrins constitute an important class of organic chromophores known to be efficient materials for optical limiting applications as a result of large excited-state absorption cross sections;[17] thus, they are potentially attractive systems for MPA-based applications. Anderson and co-workers have recently reported the synthesis of a compound (hereafter referred to as AtPtA) in which two anthracene moieties are covalently linked to a central

a)Author to whom correspondence should be addressed. Electronic mail: zgshuai@iccas.ac.cn

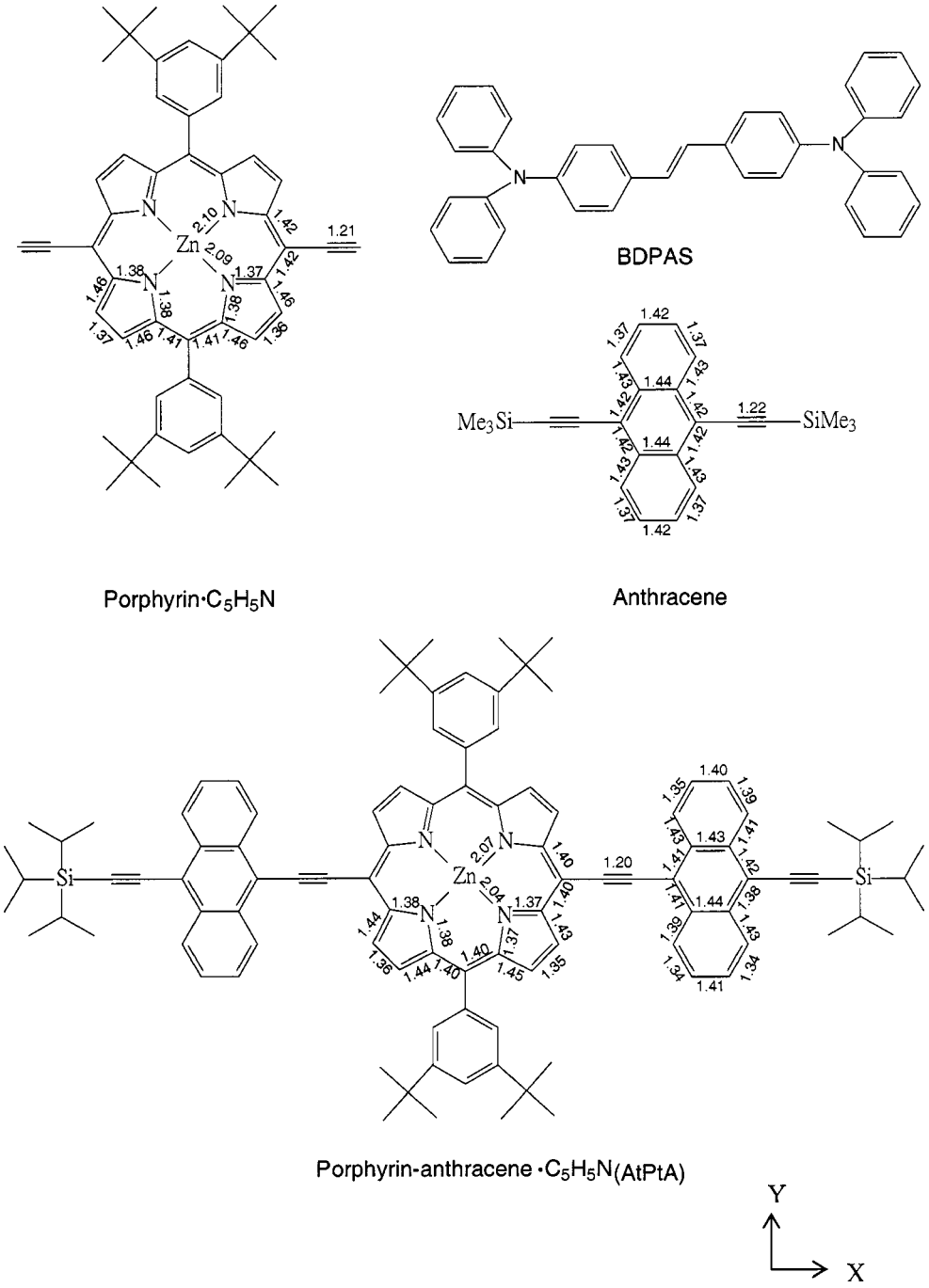

FIG. 1. Chemical structures of porphyrin, anthracene, the porphyrin-anthracene AtPtA triad, and BDPAS. Selected bond lengths (in Å) are shown for AtPtA [as obtained from x ray (Ref. 33)] and the individual molecules (as optimized at the DFT level). The *XYZ* reference frame is also shown.

porphyrin unit through two acetylenic bridges, see chemical structure in Fig. 1.

Ultrafast nonlinear absorption studies indicate that AtPtA presents sizable 2PA cross sections.[18] While modeling the two-photon absorption response of the triad structure[19] we realized that it also fulfills the requirements for 3PA in the infrared spectral domain, which is of practical importance in a number of MPA applications.[20] Thus, we explored the origin for the 3PA response in the porphyrin-anthracene triad by means of quantum-chemical calculations performed at the highly correlated coupled-cluster single and double equation of motion (CCSD-EOM) level. It is shown that the significant enhancement of the 3PA response with respect to the individual isolated chromophores arises from the strong interactions among the anthracene and porphyrin moieties, allowing for significant electronic couplings between localized and charge-transfer excitations, together with a particular excited-state energetic scheme, leading to close one-, two-, and three-photon resonances.

II. THREE-PHOTON ABSORPTION: THEORETICAL BACKGROUND

From perturbation theory, the 3PA cross section, σ_3, can be derived from the imaginary part of the fifth-order polar-

izability, $\epsilon(-\omega;\omega,\omega,-\omega,\omega,-\omega)$.[21] However, as pointed out by Cronstrand *et al.*,[15] the numerical calculation of ϵ via the full SOS approach is a formidable task. Under resonant conditions,[22,23] the 3PA cross section can be expressed as

$$\sigma_3(\omega)=\frac{4\pi^3(\hbar\omega)^3}{3n^3c^3\hbar}L^6\sum_f |T_{g\to f}|^2 \cdot\left\{\frac{\Gamma}{(E_{gf}-3\hbar\omega)^2+\Gamma^2}\right\}, \quad (1)$$

where c is the speed of light in vacuum, L denotes a local-field correction (equal to 1 for vacuum), $\hbar\omega$ is the photon energy of the incident light (a degenerate 3PA process is assumed), and Γ is a Lorentzian broadening factor (set to 0.1 eV in the calculations). $T_{g\to f}$ corresponds to the three-photon transition amplitude from the ground state to a final three-photon state $|f\rangle$, with tensor ijk elements given by[15,21]

$$T^{ijk}_{g\to f}=P_{ijk}\sum_{m,n}\frac{\langle g|\mu_i|m\rangle\langle m|\mu_j|n\rangle\langle n|\mu_k|f\rangle}{(E_{gm}-\hbar\omega-i\Gamma)(E_{gn}-2\hbar\omega-i\Gamma)}, \quad (2)$$

where E_{gm} corresponds to the excitation energy from the ground-state $|g\rangle$ to excited-state $|m\rangle$, μ_i is the component of the electric dipole operator along molecular axis i, and P_{ijk} denotes a complete permutation of the indices i, j, and k. From the general SOS expression, $\epsilon(-\omega;\omega,\omega,-\omega,\omega,-\omega)$ consists of $6!=720$ terms, among which $(3!)^2=36$ terms involve the following resonant factor:

$$\frac{1}{(E_{gm}-\hbar\omega)(E_{gn}-2\hbar\omega)(E_{gl}-3\hbar\omega)(E_{gn'}-2\hbar\omega)(E_{gm'}-\hbar\omega)}.$$

The T-tensor approach of Eqs. (1) and (2) corresponds to these 36 terms, which are relevant to the 3PA process; indeed, P_{ijk} generates exactly $3!=6$ terms, and its square (3PA) gives rise to 36 terms.

Note that, in AtPtA, the longitudinal $xxxxxx$ component of the 3PA amplitude (with the x axis oriented along the vector joining the porphyrin macrocycle to the anthracene moieties, see Fig. 1) is found to be several orders of magnitude larger than any other tensor component. In the following, only this component is therefore calculated explicitly. The three-photon absorption cross section can then be written (in $\mathrm{cm}^6\,\mathrm{s}^2/\mathrm{photon}^2$)

$$\sigma_3(\omega)=2.03\times10^{-86}(\hbar\omega)^3\frac{L^6}{n^3} \times\sum_f\left|\sum_{m,n}\frac{\langle g|\mu_x|m\rangle\langle m|\mu_x|n\rangle\langle n|\mu_x|f\rangle}{(E_{gm}-\hbar\omega-i\Gamma)(E_{gn}-2\hbar\omega-i\Gamma)}\right|^2 \cdot\left\{\frac{\Gamma}{(E_{gf}-3\hbar\omega)^2+\Gamma^2}\right\}. \quad (3)$$

For comparative purposes, the two-photon absorption (2PA) spectrum, $\sigma_2(\omega)$, was simulated using a similar approach, i.e., on the basis of the two-photon transition amplitudes $S_{g\to f}$ with the ij tensor component defined as[24]

$$S^{ij}_{g\to f}=P_{ij}\sum_m\frac{\langle g|\mu_i|m\rangle\langle m|\mu_j|f\rangle}{(E_{gm}-\hbar\omega-i\Gamma)}. \quad (4)$$

Note that for 2PA, there are four resonant terms among the 24 terms generated by permutation over the indices in a SOS picture; these four terms are accounted for in Eq. (4).

III. THEORETICAL METHODOLOGY

A proper description of high-lying excited states is essential to provide a quantitative picture for the nonlinear optical properties of conjugated systems, especially at higher order. For instance, while a single configuration interaction (SCI) formalism is in most cases reliable to describe the second-order polarizability (β),[25] a minimal description of the third-order response should include two-electron excitation contributions.[26] Since the single and double configuration interaction method is not size consistent, the calculation of γ in large molecular systems usually proceeds through a multireference single and double CI formalism[27] allowing for a better account of electron correlation effects. In this work, we apply the coupled-cluster equation of motion method with single and double excitations[28] coupled to the semiempirical intermediate neglect of differential overlap (INDO) Hamiltonian (Ref. 29) (CCSD-EOM/INDO). This method has been shown to be efficient, size consistent, and highly accurate to describe electronic excitations in conjugated systems.[30] The semiempirical parametrization allows us to carry out numerical computations for relatively large organic molecules. Ye *et al.* have shown that the CCSD-EOM/INDO approach provides reliable descriptions for the excited states of both neutral and charged olig(othiophene)s, oligo(phenylene)s, oligo(phenylene-vinylene)s, and polyenes.[31] The Ohno–Klopman potential[32] is used to describe the Coulomb repulsion terms. The active space used in the CCSD calculations includes 14 highest occupied molecular orbitals (HOMO) and 14 lowest unoccupied molecular orbitals (LUMO), both for the ground state and the excited states; by comparison to SCI results including all valence orbitals with dominant π character, such an active space was found to retain the dominant molecular orbitals in the expansion of the excited states of interest.

The chemical structures of the molecules studied in the present work are displayed in Fig. 1. The x-ray crystal struc-

ture of the $Si(Me)_3$ end-capped zinc porphyrin-anthracene (AtPtA) compound has been reported in Ref. 33 and has been used as input for the CCSD calculations here. Interestingly, the planes of the anthracene moieties were found to be twisted by 40.9° with respect to that of the Zn-porphyrin macrocycle,[33] which should allow for electronic coupling among the different units across the acetylenic bridges. The ground-state geometries for the isolated anthracene and Zn-porphyrin molecules were optimized at the density-functional theory (DFT) level with the hybrid Beck three-parameter Lee–Yang–Parr functionals and the 3-21G basis set for C, N, Si, and H and the LANL2DZ basis set for Zn, as implemented in the GAUSSIAN 03 (Ref. 34) package. From Fig. 1, we note a good agreement between the bond lengths measured by x-ray diffraction in AtPtA and those optimized at the DFT level in the anthracene and porphyrin molecules; we can thus rule out geometric effects as a possible reason for the different 3PA cross sections calculated in the crystal structure geometry of AtPtA and in the DFT equilibrium geometries of the individual units.

It should be pointed out that in our approach, the geometry optimization and the electronic excited-states structure are treated at a different level. The former is well established in computational chemistry. While for the excited states, especially when higher-lying excited states are involved, there are no much choices in methodology; after all, the system size is quite big. Such a combined approach is not so commonly practiced in computational chemistry, namely, it means that the excitation does not occur at the minimum of the molecular geometry which would be obtained in the second method. However, the complexity of the problem goes beyond the abilities of standard methods. Our previous results indicate that such a combination gives reasonable agreement with the experiments.[30,31]

To test the reliability of our approach, we have also performed theoretical calculations on 4,4′-bis(diphenylamino) preanalytical systems (BDPAS) stilbene, for which a well-resolved 3PA spectrum has been measured by Drobizhev *et al.*[35] This spectrum allows (i) a clear identification of the target–state in the 3PA process and (ii) a reliable estimate of the width (Γ) of the spectral feature, which is an essential parameter for a quantitative comparison between theory and experiment.

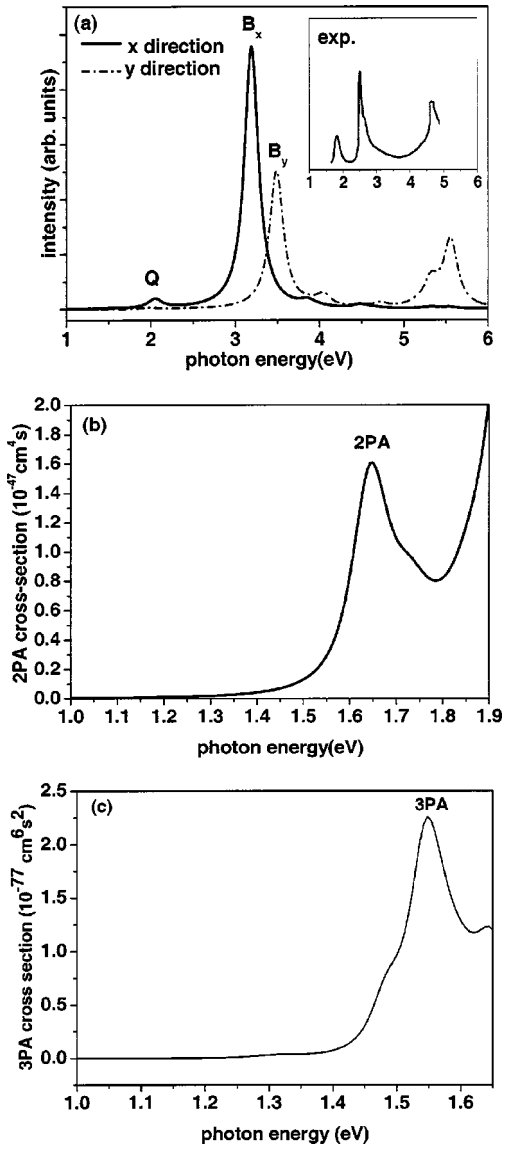

FIG. 2. (a) CCSD-polarized linear absorption spectrum of AtPtA. The solid and dashed lines correspond to polarization along the *X* and *Y* axes, respectively. The experimental spectrum is plotted in the top right corner for the sake of comparison. (b) The corresponding two-photon absorption spectrum. (c) The corresponding three-photon absorption spectrum. The main resonance features are labeled, see text for discussion.

IV. ESSENTIAL-STATE ANALYSIS OF THE THREE-PHOTON ABSORPTION RESPONSE

Before discussing the three-photon absorption response, it is useful to summarize the main features pertaining to the one- and two-photon absorption spectra (a detailed analysis will be presented elsewhere[19]), as this analysis reveals the nature of the intermediate excited states involved in the description of σ_3. The CCSD-EOM-INDO polarized linear absorption spectrum of AtPtA is shown in Fig. 2(a). Along the *x* axis (the reference framework is defined in Fig. 1), the linear spectrum is dominated by porphyrin absorptions, with optical features at 2.0 eV (weak) and 3.2 eV (strong), corresponding to the *Q* and *B* bands of isolated porphyrin, respectively, and coming from the S_2 and S_4 singlet excited states in the CCSD calculations. Although S_2 and S_4 are described primarily by an antisymmetric (destructive) combination and a symmetric (constructive) combination of the HOMO-1 to LUMO and HOMO to LUMO+1 excitations,[36] with the four frontier molecular orbitals being mostly localized on the porphyrin ring (see Table I and Fig. 3), these excited states (especially S_4) have also significant contributions from short-axis polarized electronic excitations of the anthracene units. This is clearly seen from the transition density diagrams reported in Fig. 4 (these transition charges provide a local map for the overlap between the initial—here, the ground state—and the final electronic states involved in the optical transition[37]).

The simulated *y*-polarized spectrum shows two main features at 3.5 eV (*y* component of the porphyrin *B* band) and above 5 eV (long-axis polarized anthracene absorption);

TABLE I. Main configurations and CI coefficients (with amplitudes larger than 0.3) for the essential one-, two-, and three-photon excited states of AtPtA.

Excited state	Configurations and CI coefficient	
S_2	HOMO-1→ LUMO	0.69
	HOMO→ LUMO+1	0.61
S_4	HOMO→ LUMO+1	0.56
	HOMO-1→ LUMO	−0.52
	HOMO-2→ LUMO+2	−0.38
S_6	HOMO-1→ LUMO+6	−0.63
	HOMO-1→ LUMO+2	0.45
S_{31}	HOMO-1→ LUMO+3	0.44
	HOMO-12→ LUMO	0.34
	(HOMO-3,HOMO)→(LUMO+1,LUMO+2)	0.31
S_{41}	HOMO-3→ LUMO	0.52
	HOMO-3→ LUMO+3	−0.35
	HOMO-1→ LUMO+3	−0.35

these play, however, a minor role in the three-photon absorption response and will not be discussed further. Finally, we note that, although the theoretical transition energies are significantly overestimated, the overall shape of the one-photon absorption spectrum compares very well to the experimental spectrum reported in Ref. 33, which is depicted in Fig. 2(a) for comparison; the experimental spectrum is characterized by (i) bands peaking at ~1.8 eV (weak) and ~2.6 eV (strong) and associated to the porphyrin *Q* and *B* bands, respectively; and (ii) the emergence of an additional intense band at ~4.7 eV assigned to anthracene localized excitations. It is worth stressing that the oscillator strength associated with the *Q* band is significantly enhanced in AtPtA as compared to Zn porphyrin (not shown), a feature that arises from partial wave-function delocalization between the porphyrin and anthracene units, see the analysis of the transition density diagrams above.

In the spectral range below linear absorption (i.e., below absorption into the *Q* band at ~2 eV), the 2PA spectrum of AtPtA, displayed in Fig. 2(b), is dominated by a single peak at ~1.65 eV, associated with a singlet excited state (S_6)

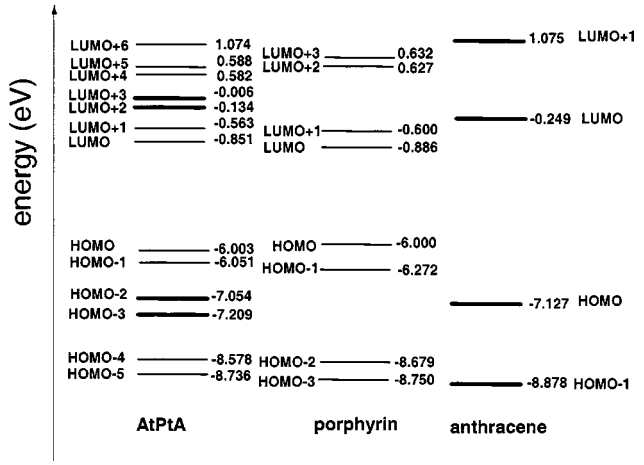

FIG. 3. Schematic representation of the one-electronic structure of AtPtA, porphyrin, and anthracene from INDO calculations. The bold lines represent molecular orbitals mostly localized on anthracene, the plain lines orbitals mostly localized on porphyrin.

located at ~3.3 eV above the ground state and coupled through significant transition dipole moments to S_2 and S_4, see Fig. 5. As in the case of S_4 (the dominant one-photon state), the lowest two-photon excited state involves both porphyrin and (smaller) anthracene contributions; the S_6 excited-state wave function is indeed primarily described by electronic transitions from the HOMO-1 to the LUMO+6 and (to a lesser extent) LUMO+2 orbitals, which are mostly confined on the central porphyrin macrocycle and anthracene end caps, respectively (Table I, Fig. 3). As a result, the $S_2 \rightarrow S_6$ and $S_4 \rightarrow S_6$ excitations involve a reorganization of the electron density over the whole AtPtA structures (as illustrated by the transition densities diagrams on Fig. 4); the amplitudes are small, which translates into transition dipoles of intermediate size. The (orientationally averaged) 2PA cross section (characteristic of isotropic samples) at the resonance (~1.65 eV) is calculated from Eq. (4) to be $320 \times 10^{-50}\,\mathrm{cm}^4\,\mathrm{s}$ (the longitudinal component amounts to $1600 \times 10^{-50}\,\mathrm{cm}^4\,\mathrm{s}$). For the sake of comparison, we also computed the (orientationally averaged) 2PA cross section from the SOS expression of $\mathrm{Im}(\gamma(-\omega;\omega,\omega,-\omega))$, which amounts to $340 \times 10^{-50}\,\mathrm{cm}^4\,\mathrm{s}$. The (slight) deviation between the results obtained by the two methods arises from the fact that the SOS results also include contributions from non-two-photon resonant terms. The latter are key to understand the static third-order susceptibility,[29] but are not as relevant for the 2PA or 3PA resonant behaviors.

Figure 2(c) shows the simulated frequency-dependent 3PA spectrum of AtPtA in a spectral range for which the molecule is transparent for both one- and two-photon absorption (however, due to the simple treatment used here to account for line broadening, the residual lower-order absorption cannot be quantified). As in the case of 2PA, the 3PA spectrum below 1.65 eV is characterized by the presence of a single strong resonance at about 1.5 eV. From Eq. (3), the longitudinal component of the 3PA absorption cross section at this resonance is $\sim 2.3 \times 10^{-77}\,\mathrm{cm}^6\,\mathrm{s}^2/\mathrm{photon}^2$.

As indicated above, we have also calculated the 3PA coefficient of BDPAS,[35] which has been measured by Drobizhev *et al.* Applying the same methodology leads to an *xxxxxx* component of the 3PA cross section (with *x* being the charge-transfer axis) that is more than two orders of magnitude larger than the other components. It amounts to $2.88 \times 10^{-80}\,\mathrm{cm}^6\,\mathrm{s}^2/\mathrm{photon}^2$ for a fundamental energy of 1.24 eV (3PA into the S_1 state). This is three orders of magnitude lower than in AtPtA.

To allow a comparison with experimental spectra in solution, it is necessary to take into account spatial averaging over all possible molecular orientations and the local-field corrections (note that solvent-induced changes of transition energies and dipole moments go beyond the scope of the present contribution). According to Cronstrand *et al.*,[15] orientational averaging contributes a factor of 2/35 or 1/7 (when a single component dominates the 3PA tensor), in the case of circular or linear polarization, respectively. Within the simple Lorentz model, the local-field correction is $L = (n^2+2)/3$. For dichloromethane (with a refractive index $n = 1.4242$), one obtains $L^6 = 5.86$ and L^6/n^3 [the solvent-related term entering into Eq. (3)] becomes 2.03. Thus, these

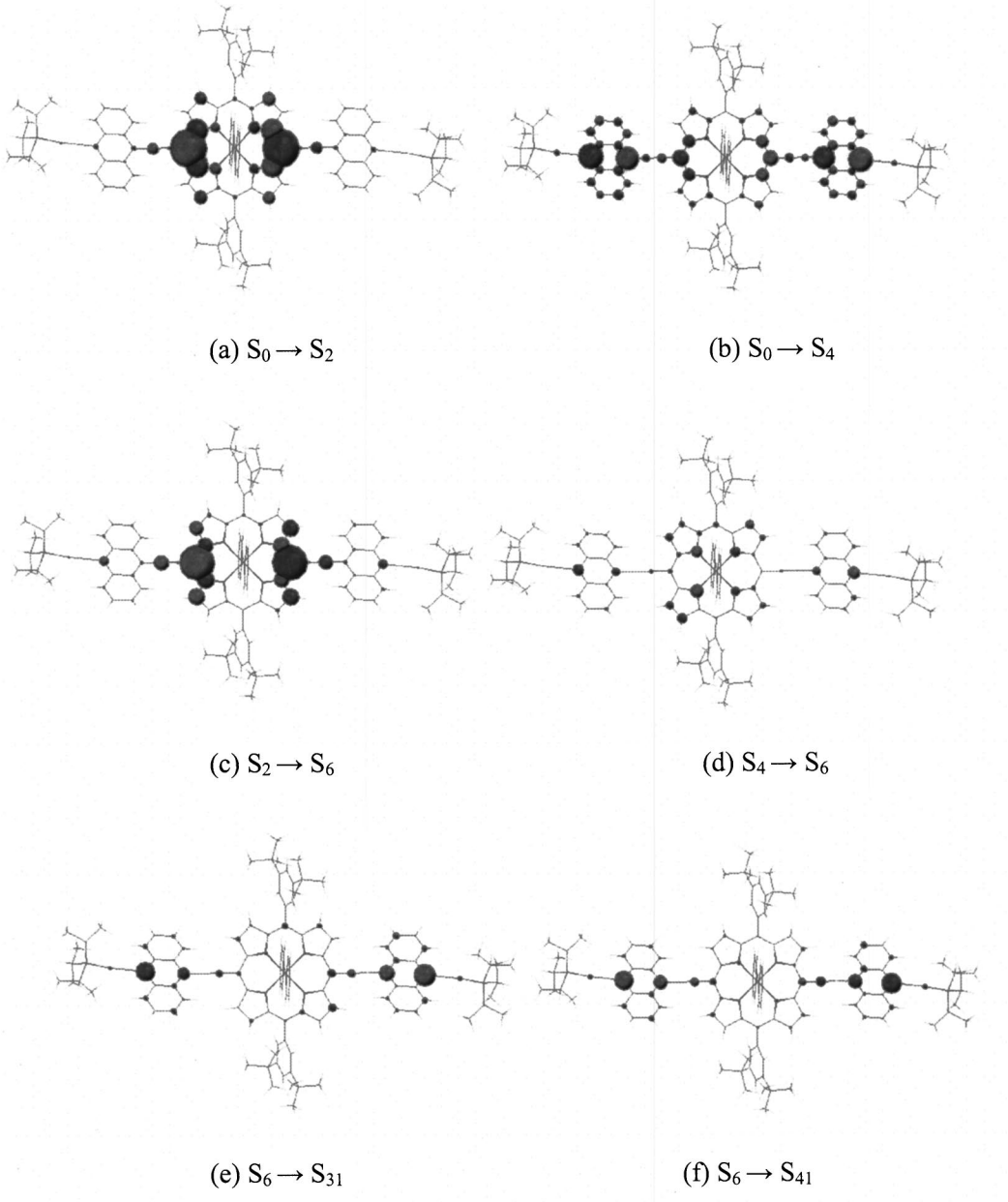

FIG. 4. Transition density diagrams associated to the electronic excitations dominating the description of the three-photon absorption response. For the sake of clarity, the transition densities have been magnified by relative ratios of 10 for (a) and (b); 30 for (c); 40 for (d), (e), and (f).

combined effects contribute overall factors of ~0.12 and ~0.30 for the two light-polarization conditions. The theoretical 3PA value for BDPAS in an isotropic dichloromethane solution and for a linearly polarized light (i.e., experimental conditions in Ref. 35) is then estimated to be $\sim 8.6 \times 10^{-81}\,\mathrm{cm}^6\,\mathrm{s}^2/\mathrm{photon}^2$, at the theoretical peak position of 1.24 eV. This is very close to the experimental value of $5 \times 10^{-81}\,\mathrm{cm}^6\,\mathrm{s}^2/\mathrm{photon}^2$ at the experimental peak position of 1.06 eV (Ref. 35) (note that our choice of 0.1 eV for the damping Γ translates into a peak width of 0.3 eV when plotting the 3PA spectrum as a function of state energy, which is consistent with the measurements in Ref. 35).

We have also calculated the 3PA cross section for the individual anthracene and porphyrin molecules; looking at the same frequency range, these are found to be two orders of magnitude smaller than in the triad molecule. In order to understand the microscopic mechanism for such a large enhancement of the 3PA cross section in the triad molecule, we have analyzed the dominant channels contributing to $T_{g\rightarrow f}$ and identified the involved excited states, see Fig. 5 (note that the different pathways for σ_3 result from all possible combinations of these channels). As expected from the discussion of the one- and two-photon spectra above, S_6 is an essential intermediate state, i.e., the three-photon response involves large contributions from channels such as $|S_0\rangle \rightarrow |S_m\rangle \rightarrow |S_6\rangle \rightarrow |S_f\rangle$, where S_m stands for S_2 or S_4 and S_f corresponds to S_{31} or S_{41} (plus additional smaller contributions in the same energy range). S_{31} and S_{41} are two close-lying three-photon excited states. The dominant electronic configuration to the wave-function expansion for S_{31} is a single electron promotion from HOMO-1 to LUMO+3, while the HOMO-3 to LUMO transition provides the largest

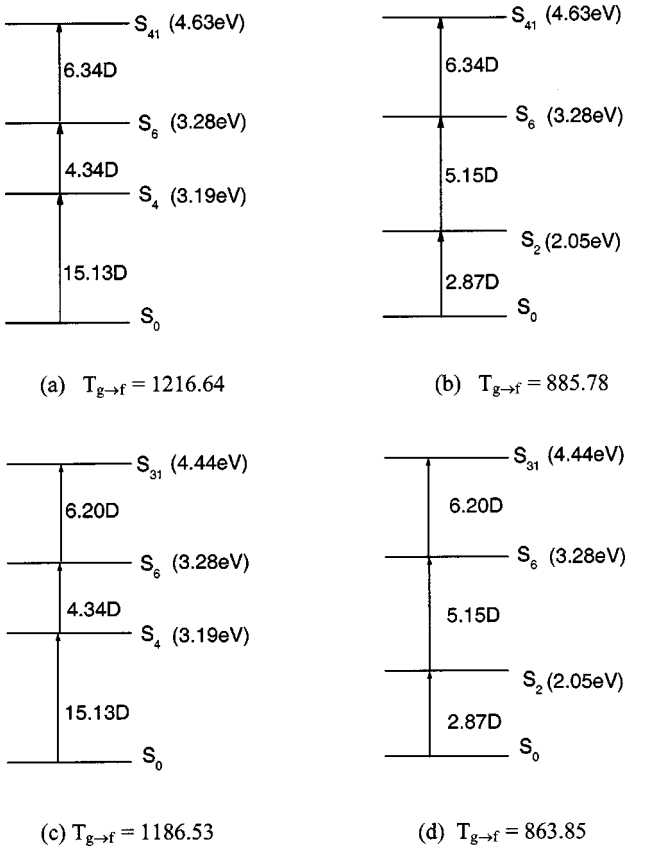

FIG. 5. Schematic picture of the relevant four dominant channels to the 3PA cross section at 1.5 eV, showing the transition energies and dipole moments between the involved excited states. The associated $|T_{g\to f}|$ values are listed below.

contribution to the S_{41} wave function (Table I, Fig. 3); these two transitions correspond to charge-transfer excitations from porphyrin to anthracene and vice versa, respectively (note, however, that these excited-state wave functions are very disperse with a large number of small contributions, see Table I). The magnitude of the overall charge transfer amounts to $\sim 0.7\ |e|$ in both S_{31} and S_{41}. Because of such a dominant charge-transfer character, these excited states have vanishingly small oscillator strength to the ground state, and hence do not appear in the linear absorption spectrum; however, they are characterized by sizable transition dipole moments to the dominant two-photon state S_6 (Fig. 5), with major contributions on the anthracene moieties (Fig. 4).

The large enhancement of 3PA cross section in the triad molecule can hence be explained as follows:

(i) The strong coupling between the porphyrin and anthracene moieties that gives rise to relatively large dipole matrix elements between the following pairs of states: S_0 with S_2 and S_4 (B band), S_2 and S_4 with S_6 (2PA state), and S_6 with S_{31} and S_{41} (3PA target states).

(ii) The closeness of the one-, two-, and three-photon resonances that lead to small detuning factors; for instance, the photon energy for the three-photon resonance is detuned by only 0.5 eV relative to the one-photon resonance into the Q band, $E_{S_2}-\hbar\omega \sim 0.5$ eV. At the same photon energy, it is also close to the 2PA resonance into S_6, $E_{S_6}-2\hbar\omega \sim 0.2$ eV. These two energy differences enter into the denominator in Eq. (3) and their small values result in a significant enhancement of the 3PA cross section. (In this context, one, however, has to keep in mind that, if one-, two-, and three-photon states lie too close in energy, in practical applications, higher-order nonlinear absorption processes will be obscured by lower-order ones.) Finally, it is interesting to note that (i) in spite of a less favorable energy factor, the B-band (S_4) contribution to 3PA is comparable to that of the Q band (S_2), due to the larger transition dipole moment to the ground state; and (ii) although larger transition moments are involved, the three-photon resonances associated with either the B band (S_4) or the Q band (S_1 and S_2) have much smaller intensity than those to the S_{31} and S_{41} excited states [because these lead to larger detuning factors at the denominator in Eq. (3) and involve a smaller number of possible pathways].

V. CONCLUSIONS

To summarize, we have investigated the three-photon absorption response of a porphyrin-anthracene triad (AtPtA) using a highly correlated CCSD-EOM/INDO method. The 3PA cross section of AtPtA has been found to be two orders of magnitude larger than those of the individual entities and about three orders of magnitude larger than the values reported for BDPAS.

Such an enhancement of the 3PA response is associated to the presence of three-photon states with a predominant intramolecular charge-transfer character, which show large transition dipole moments to a major two-photon excited state delocalized over the porphyrin and anthracene moieties. The latter state itself is strongly coupled to the excited states leading to the porphyrin Q and B bands that dominate the linear absorption spectrum. In a simplified picture, the sequence of excitations $S_0 \to (S_2/S_4)$, $(S_2/S_4) \to S_6$, and $S_6 \to (S_{31}/S_{41})$ can be regarded as progressively shifting the electronic density from the central porphyrin macrocycle to the external anthracene chromophores. This, together with the particular excited-state energy scheme leading to closely lying one-, two-, and three-photon resonances, provides the mechanism for the enhanced 3PA cross section in the triad structure. Although this theoretical prediction has still to be confirmed experimentally, it paves the way towards the design of molecular architectures for 3PA applications. In particular, it would be interesting to explore the 3PA response of 2PA active materials; such a study is currently in progress.

ACKNOWLEDGMENTS

The authors are grateful for the stimulating discussions with Yi Luo and Mikhail Drobizhev. This work is supported by National Science Foundation of China (Grant Nos. 20420150034, 90203015, and 90301001), the Ministry of Sciences and Technology of China, and the CNIC-supercomputer center of the Chinese Academy of Sciences. One of the authors (D.B.) is a Senior Research Associate of the Belgian National Science Foundation (FNRS); the work in Mons is partly supported by the Belgian Federal Government Office for Scientific Technological and Cultural Affairs

in the framework of the InterUniversity Attraction Pole program P5/03. The work at Georgia Tech is supported in part by the National Science Foundation through the STC Program under Award No. DMR-0120967, DARPA, and the IBM Shared University Research Program.

[1] G. S. He, G. C. Xu, P. N. Prasad, B. A. Reinhardt, J. C. Bhatt, and A. G. Dillard, Opt. Lett. **20**, 435 (1995).
[2] A. Mukherjee, Appl. Phys. Lett. **62**, 3423 (1993).
[3] W. Denk, J. H. Strickler, and W. W. Webb, Science **248**, 73 (1990).
[4] W. E. Moerner and S. M. Silence, Chem. Rev. (Washington, D.C.) **94**, 127 (1994).
[5] D. A. Parthenopoulos and P. M. Rentzepis, Science **245**, 843 (1989).
[6] H. Stiel, K. Teuchner, A. Paul, W. Fveyer, and D. Leupold, J. Photochem. Photobiol., A **80**, 289 (1994).
[7] M. Drobizhev, A. Karotki, M. Kruk, Y. Dzenis, A. Rebane, F. Meng, E. Nickel, and C. W. Spangler, Proc. SPIE **5211**, 63 (2003).
[8] G. S. He, J. D. Bhawalkar, and P. N. Prasad, Opt. Lett. **20**, 1524 (1995).
[9] J. D. Bhawalkar, G. S. He, and P. N. Prasad, Opt. Commun. **119**, 587 (1995).
[10] G. S. He, P. P. Markowicz, T. C. Lin, and P. N. Prasad, Nature (London) **415**, 767 (2002).
[11] G. Y. Zhou, X. M. Wang, D. Wang, Z. S. Shao, and M. H. Jiang, Appl. Opt. **41**, 1120 (2002); C. L. Zhan, D. H. Li, D. Q. Zhang *et al.*, Chem. Phys. Lett. **353**, 138 (2002); J. X. Zhang, Y. P. Cui, C. X. Xu, M. L. Wang, and J. Z. Liu, Jpn. J. Appl. Phys. **41**, 462 (2002); D. Y. Wang, C. L. Zhan, Y. Chen, Y. J. Li, Z. Z. Lu, and Y. X. Nie, Chem. Phys. Lett. **369**, 621 (2003).
[12] H. F. Hameka, Physica (Utrecht) **32**, 779 (1966).
[13] V. Galasso, J. Chem. Phys. **92**, 2495 (1990).
[14] G. Marconi and P. R. Salvi, Chem. Phys. Lett. **193**, 481 (1992).
[15] P. Cronstrand, Y. Luo, P. Norman, and H. Ågren, Chem. Phys. Lett. **375**, 233 (2003).
[16] B. J. Orr and J. F. Ward, Mol. Phys. **20**, 513 (1971).
[17] G. E. O'Keefe, G. J. Denton, E. J. Harvey, R. T. Phillips, R. H. Friend, and H. L. Anderson, J. Chem. Phys. **104**, 805 (1996).
[18] M. Drobizhev, A. Karotki, M. Kruk, and A. Rebane, Chem. Phys. Lett. **355**, 175 (2002).
[19] L. Y. Zhu *et al.* (unpublished).
[20] T. Kogej, D. Beljonne, F. Meyers, J. W. Perry, S. R. Marder, and J. L. Brédas, Chem. Phys. Lett. **298**, 1 (1998).
[21] W. L. Peticolas, Annu. Rev. Phys. Chem. **18**, 233 (1967).
[22] R. L. Sutherland, *Handbook of Nonlinear Optics*, 2nd ed. (Marcel Dekker, New York, 2003), p. 591, where 3PA coefficient γ is presented. According to Bhawalkar *et al.* (Ref. 23), we convert the γ (expression in cgs) to 3PA cross section as $\sigma_3 = \gamma(\hbar\omega)^2/N5!$, which is exactly Eq. (1), where N is the molecular number per volume, factorial 5! comes from the difference between Taylor expansion and power expansion, namely, factorials 2!, 3!, 4!, and 5! for second, third, fourth, and fifth nonlinear polarizabilities, respectively.
[23] J. D. Bhawalkar, G. S. He, and P. N. Prasad, Rep. Prog. Phys. **59**, 1041 (1996); P. Cronstrand, Ph.D. thesis, Royal Institute of Technology, 2004.
[24] P. Norman, Y. Luo, and H. Ågren, Chem. Phys. Lett. **296**, 8 (1998).
[25] F. Meyers, S. R. Marder, B. M. Pierce, and J. L. Brédas, J. Am. Chem. Soc. **116**, 10703 (1994).
[26] B. M. Pierce, J. Chem. Phys. **91**, 791 (1989); Z. Shuai and J. L. Brédas, Phys. Rev. B **44**, 5962 (1991).
[27] R. J. Buenker and S. D. Peyerimhoff, Theor. Chim. Acta **35**, 33 (1974); P. Tavan and K. Schulten, J. Chem. Phys. **85**, 6602 (1986); Z. Shuai, D. Beljonne, and J. L. Brédas, J. Chem. Phys. **97**, 1132 (1992).
[28] J. F. Stanton and R. J. Bartlett, J. Chem. Phys. **98**, 7029 (1993); D. L. Comeau and R. J. Bartlett, Chem. Phys. Lett. **207**, 414 (1993); R. J. Bartlett and J. F. Stanton, Rev. Comput. Chem. **5**, 65 (1994).
[29] J. Ridley and M. C. Zerner, Theor. Chim. Acta **32**, 111 (1973).
[30] Z. Shuai and J. L. Brédas, Phys. Rev. B **62**, 15452 (2000); A. Ye, Z. Shuai, and J. L. Brédas, *ibid.* **65**, 045208 (2002).
[31] A. Ye, D. Beljonne, Z. Shuai, and J. L. Brédas, J. Chem. Phys. (in press).
[32] K. Ohno, Theor. Chim. Acta **2**, 219 (1964); G. Klopman, J. Am. Chem. Soc. **86**, 4550 (1964).
[33] P. N. Taylor, A. P. Wylie, J. Huuskonen, and H. L. Anderson, Angew. Chem., Int. Ed. **37**, 986 (1998).
[34] M. J. Frisch, G. W. Trucks, H. B. Schlegd *et al.*, GAUSSIAN 03, Gaussian Inc., Carnegie PA, 2003.
[35] M. Drobizhev, A. Karotki, M. Kruk, Y. Dzenis, A. Rebane, Z. Suo, and C. W. Spangler, J. Phys. Chem. B **108**, 4221 (2004).
[36] I. M. Blake, H. L. Anderson, D. Beljonne, J. L. Brédas, and W. Clegg, J. Am. Chem. Soc. **102**, 10764 (1998).
[37] D. Beljonne, J. Cornil, R. Silbey, P. Millié, and J. L. Brédas, J. Chem. Phys. **112**, 4749 (2000); J. P. Calbert, ZOA V2.5, http://zoa.freeservers.com